Organic & Biomolecular Chemistry

Accepted Manuscript

ROYAL SOCIETY OF CHEMISTRY

www.rsc.org/obc

Cite this: DOI: 10.1039/c0xx00000x

www.rsc.org/xxxxxx

ARTICLE TYPE

Photoinduced changes in hydrogen bonding patterns of 8-thiopurine nucleobase analogues in a DNA strand

Kunihiko Morihiro,[a,b] Tetsuya Kodama,[c] Shohei Mori[a] and Satoshi Obika*[a,b]

Received (in XXX, XXX) Xth XXXXXXXXX 20XX, Accepted Xth XXXXXXXXX 20XX

DOI: 10.1039/b000000x

Hydrogen bonds (H-bonds) formed between nucleobases play an important role in the construction of various nucleic acid structures. The H-donor and H-acceptor pattern of a nucleobase is responsible for selective and correct base pair formation. Herein, we describe an 8-thioadenine nucleobase analogue and an 8-thiohypoxanthine nucleobase analogue with a photolabile 6-nitroveratryl (NV) group on the sulfur atom (**SA**^{NV} and **SH**^{NV}, respectively). Light-triggered removal of the NV group causes tautomerization and a change in the H-bonding pattern of **SA**^{NV} and **SH**^{NV}. This change in H-bonding pattern has a strong effect on base recognition by 8-thiopurine nucleobase analogues. In particular, base recognition by **SH**^{NV} is clearly shifted from guanine to adenine upon photoirradiation. These results show that a photoinduced change in H-bonding pattern is a unique strategy for manipulating nucleic acids assembly with spatiotemporal control.

Introduction

The complementarity of natural A-T and G-C base pairs in DNA is the principal mechanism for the preservation and flow of genetic information. The hydrogen-bonding (H-bonding) patterns of the four natural nucleobases play an important role in the selective and correct formation of base pairs. These H-bonding interactions can result in the formation of higher order complexes of nucleic acids, depending on the sequence. Therefore, the control of H-bonding interactions using external stimuli is important for regulating biological processes, and for the possibility of developing unique DNA-based molecular machines. Various external stimuli have been used to this end; light is an ideal trigger because the timing, location, intensity of the irradiation can be easily controlled. Among such strategies, nucleobase caging strategies involving the installation of a photolabile group are very important. Photolabile caging groups perturb the H-bonding capabilities of the nucleobases. Photoirradiation reinstates the H-bonding capabilities and allows nucleobase interaction in the "OFF to ON" direction. Nucleobase-caged nucleosides can be widely used for the photoregulation of antisense oligodeoxynucleotides (ODNs),[1,2] siRNAs,[3,4] aptamers,[5] ribozymes[6,7] and deoxyribozymes,[8,9] diagnostic ODNs,[10] DNA architectures,[11] and DNA logic gates.[12,13]

Recently, we reported the synthesis and properties of a unique light-responsive nucleobase analogue derived from 2-mercaptobenzimidazole (**SB**^{NV}) (Fig. 1a).[14] **SB**^{NV} is modified with a photolabile 6-nitroveratryl (NV) group,[15] and the nitrogen at the 3-position serves as an H-acceptor (A). **SB**^{NV} can selectively form a base pair with guanine even before photoirradiation, unlike conventional caged nucleobases. Light-triggered removal of the NV group causes tautomerization of the nucleobase, and changes the role of the 3-nitrogen atom from H-A to H-donor (D). Following this change in H-bonding pattern, base recognition by **SB**^{NV} can be shifted from guanine to adenine. We also demonstrated that a light-triggered strand exchange reaction targeting different mRNA fragment sequences could be achieved using ODNs containing **SB**^{NV}. These results indicate

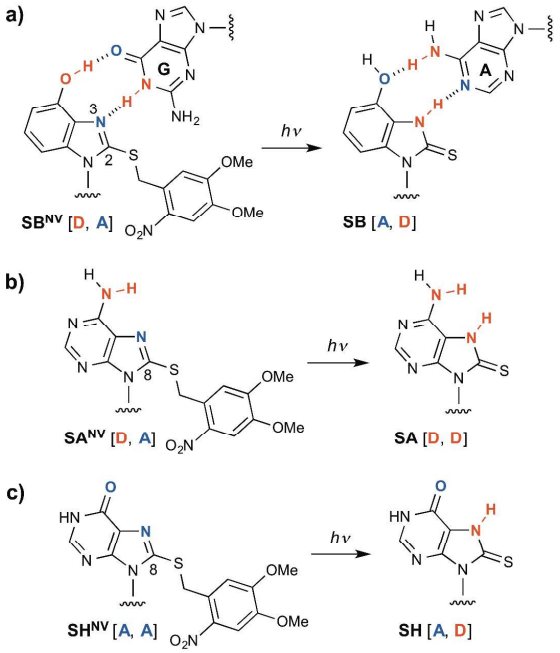

Fig. 1 (a) Change in base recognition by **SB**^{NV} upon photoirradiation. (b) Photoinduced changes in hydrogen bonding patterns of **SA**^{NV} and (c) **SH**^{NV}.

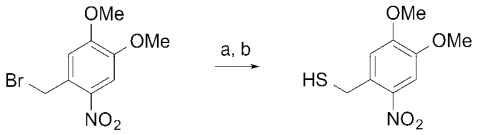

Scheme 1 Preparation of 6-nitroveratrylthiol **2**. *Reagents and conditions*: (a) KSAc, THF, rt; (b) conc. HCl aq., MeOH, 60 °C, 94% over two steps.

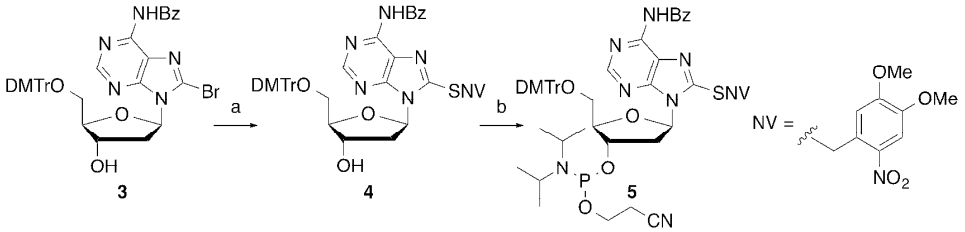

Scheme 2 Preparation of the phosphoramidites bearing $\mathbf{SA}^{\mathbf{NV}}$. *Reagents and conditions*: (a) **2**, K_2CO_3, DMF, rt, 52%; (b) (iPr$_2$N)P(Cl)O(CH$_2$)$_2$CN, iPr$_2$NEt, MeCN, rt, 77%

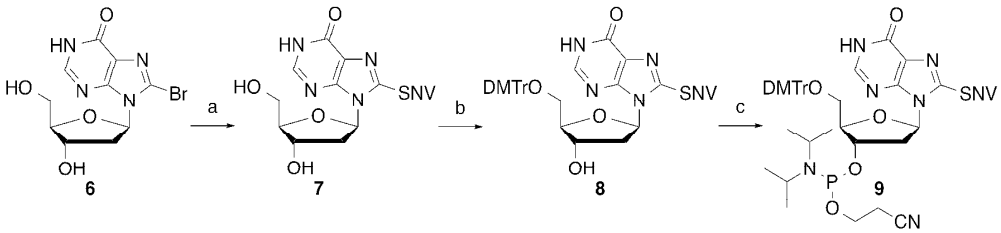

Scheme 3 Preparation of the phosphoramidites bearing $\mathbf{SH}^{\mathbf{NV}}$. *Reagents and conditions*: (a) **2**, K_2CO_3, DMF, rt, 25%; (b) DMTrCl, pyridine, rt, 85%; (c) (iPr$_2$N)P(Cl)O(CH$_2$)$_2$CN, iPr$_2$NEt, MeCN, rt, 74%.

that a photoinduced change in the H-bonding pattern of a nucleobase is a good strategy for manipulating nucleic acid assemblies in a spatially and temporally controlled manner. In this paper, to further investigate the effect of this change in H-bonding pattern of nucleobases on base recognition ability, we designed new light-responsive nucleoside analogues bearing the NV group: 8-thioadenine and 8-thiohypoxantine ($\mathbf{SA}^{\mathbf{NV}}$ and $\mathbf{SH}^{\mathbf{NV}}$, respectively; Fig. 1b). 8-Thiopurine analogues should preferentially adopt the *syn* conformation about the glycosidic bond due to steric repulsion between the C8-sulfur atom and the 4'-oxygen atom in the *anti* conformer.[16,17] $\mathbf{SA}^{\mathbf{NV}}$ and $\mathbf{SH}^{\mathbf{NV}}$ also should adopt the *syn* conformation and use the H-A and H-D Hoogsteen face to contact the target base. The H-bonding pattern of $\mathbf{SA}^{\mathbf{NV}}$ and $\mathbf{SH}^{\mathbf{NV}}$ at the Hoogsteen face would thus be changed from [D, A] to [D, D] and [A, A] to [A, D], respectively (Fig. 1). T_m evaluation of modified ODNs revealed that photoinduced changes in H-bonding patterns of 8-thiopurine nucleobase analogues have a pronounced effect on base recognition abilities.

10 5'-d(TCGTTT**SA**$^{\mathbf{NV}}$TTGCG)-3'
11 5'-d(TCGTTT**SH**$^{\mathbf{NV}}$TTGCG)-3'
12 5'-d(TCGTTTA TTGCG)-3'
13 5'-d(TCGTTTG TTGCG)-3'
14 3'-d(AGCAAAA AACGC)-5'
15 3'-d(AGCAAAG AACGC)-5'
16 3'-d(AGCAAAC AACGC)-5'
17 3'-d(AGCAAAT AACGC)-5'

Fig. 2 ODN sequences used in this study.

Results and discussion

The synthesis of the phosphoramidites bearing $\mathbf{SA}^{\mathbf{NV}}$ and $\mathbf{SH}^{\mathbf{NV}}$ as a nucleobase are summarized in Scheme 1. 6-Nitroveratrylthiol (**2**) was prepared from 6-nitroveratrylbromide (**1**) (Scheme 1) and subjected to reaction with 8-bromo-2'-deoxyadenosine derivative (**3**)[18] to afford **4** (Scheme 2). Phosphitylation at the 3'-hydroxyl group provided $\mathbf{SA}^{\mathbf{NV}}$-phosphoramidite **5**. For the preparation of $\mathbf{SH}^{\mathbf{NV}}$-phosphoramidite **9**, 8-bromoinosine (**6**)[19] was treated with **2** to give **7** (Scheme 3). Tritylation of the primary hydroxyl group in **7** and phosphitylation of the secondary hydroxyl group provided phosphoramidite **9**. Amidite blocks **5** and **9** were applied to an automated DNA synthesizer to incorporate $\mathbf{SA}^{\mathbf{NV}}$ and $\mathbf{SH}^{\mathbf{NV}}$ into ODNs. $\mathbf{SA}^{\mathbf{NV}}$ and $\mathbf{SH}^{\mathbf{NV}}$ were incorporated in the middle of the pyrimidine (T) strand of ODN **10** and ODN **11**. After cleavage from the resin and purification by reversed-phase (RP) HPLC, the structure of each ODN was confirmed by MALDI-TOF MS analysis. The sequence of each ODN used in this study is shown in Fig. 2.

The photoreactivity of $\mathbf{SA}^{\mathbf{NV}}$ and $\mathbf{SH}^{\mathbf{NV}}$ in a DNA strand was investigated by RP-HPLC analysis using ODN **10** and ODN **11**. When irradiated at 365 nm at 37 °C, ODN **10** and ODN **11** gradually disappeared. MALDI-TOF MS showed that the resulting ODNs were **SA**-/**SH**-ODNs and confirmed that the NV

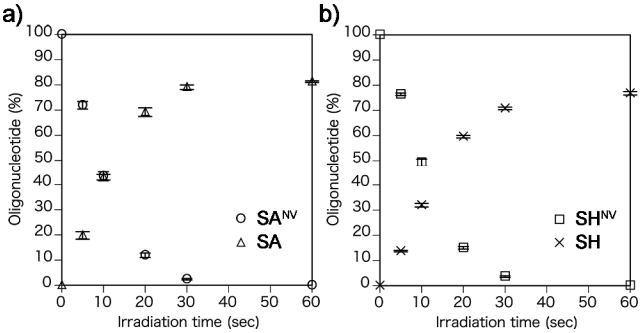

Fig. 3 Time course conversion of (a) $\mathbf{SA}^{\mathbf{NV}}$ to **SA** in ODN **10** and (b) $\mathbf{SH}^{\mathbf{NV}}$ to **SH** in ODN **11** by photoirradiation. Conditions: each ODN (0.1 nmol, 10 μM), sodium phosphate buffer (pH 7.2, 25 mM). Irradiation (365 nm) was performed at rt. Error bars indicate standard deviation (n = 3).

group of **SA**^{NV} and **SH**^{NV} was efficiently removed. Fig. 3 shows the percentage of the remaining **SA**^{NV}-/**SH**^{NV}- and resulting **SA**-/**SH**-ODNs at several irradiation time points. The photoreaction was complete within 60 sec for both ODNs, and the yield of NV-removed ODNs was estimated from the HPLC peak area to be about 80%.

The effects of photoinduced changes in H-bonding pattern of **SA**^{NV} and **SH**^{NV} on their base recognition ability were examined by measuring the T_m values of DNA duplexes containing ODN **10** and ODN **11** (Table 1). ODN **10** and ODN **11** were individually hybridized to four ODNs, generating eight distinct duplexes in which each nucleobase analogue was paired with all possible natural nucleobases. For comparison, naturally matched duplexes containing the A:T and G:C base pairs in the same position were also examined. The duplex containing the **SA**^{NV}:G pair showed the highest T_m value of all the combinations of **SA**^{NV} with other nucleobases ($\Delta T_m \geqq 3$ °C). The **SA**^{NV}:G pair was slightly less stable than natural base pairs, and similar to the stability of the G:T wobble base pair. After photoirradiation at 365 nm for 5 min, **SA** showed the highest affinity towards thymine ($\Delta T_m \geqq 4$ °C); however, the T_m values of duplexes containing **SA** are, on the whole, low ($T_m \leqq 32$ °C). **SH**^{NV} in ODN **11** showed the highest affinity towards guanine, similar to **SA**^{NV} ($\Delta T_m \geqq 4$ °C). The T_m value of the duplex containing the **SH**^{NV}:G base pair was also slightly lower than that of natural duplexes. In contrast, after irradiation, the preferred base-pairing partner for **SH**^{NV} clearly changed to adenine ($\Delta T_m \geqq 8$ °C). Notably, the stability of **SH**:A was comparable to that of the natural A:T base pair. These results suggest that photoirradiation induces a change in base recognition by **SH**^{NV} from guanine to adenine. Fig. 4 illustrates the changes in the UV melting profiles of ODN-**11**-formed DNA duplexes and clearly indicates that the change in base recognition by **SH**^{NV} is triggered by photoirradiation.

Table 1. T_m values of DNA duplexes[a]

5′-d(GCGTT**X**TTTGCT)-3′
3′-d(CGCAA**Y**AAACGA)-5′

Duplex	**X**:**Y**	T_m (°C) UV (–)	T_m (°C)[b] UV (+)
10:**14**	**SA**^{NV}:A	26	24
10:**15**	**SA**^{NV}:G	35	28
10:**16**	**SA**^{NV}:C	24	26
10:**17**	**SA**^{NV}:T	32	32
11:**14**	**SH**^{NV}:A	31	39
11:**15**	**SH**^{NV}:G	35	26
11:**16**	**SH**^{NV}:C	30	31
11:**17**	**SH**^{NV}:T	26	28
12:**17**	A:T	41	41
13:**16**	G:C	43	43
12:**15**	A:G (mismatch)	33	33
12:**16**	A:C (mismatch)	29	29
13:**14**	G:A (mismatch)	32	32
13:**17**	G:T (wobble)	35	35

[a] Conditions: each ODN (4.0 μM), NaCl (20 mM), sodium phosphate buffer (10 mM, pH 7.2). [b] T_m values of DNA duplexes after irradiation (365 nm) at 37 °C for 5 min.

Although further conclusive experiments such as NMR or X-ray structural analysis are needed to elucidate the precise base pair structures, the results of the T_m measurements suggest that **SA**^{NV} and **SH**^{NV} recognize guanine via two H bonds on the Hoogsteen face, as shown in Fig. 5. The stabilities of the **SA**^{NV} and **SH**^{NV}:G base pairs were slightly lower than that of the natural base pairs. It would appear that steric repulsion between the 8-sulfur atom in **SA**^{NV} and the 2-amino group in guanine decreases the stability of the **SA**^{NV}:G pair (Fig. 5a). This observation is consistent with previous reports showing that the base pair between 2-thiouracil and 2,6-diaminopurine is significantly destabilized because of steric hindrance.[20,21] Also, **SH**^{NV} may form a wobble pair with guanine similar to the U:G mismatch pair commonly found in RNA[22] (Fig. 5b); therefore, the **SH**^{NV}:G pair is less stable than natural base pairs. Light-induced changes in H-bonding patterns have profound effects on the base recognition abilities of 8-thiopurine nucleobase analogues. ODN containing **SA** showed low recognition ability toward any nucleobase; this can be explained by the fact that **SA** has an H-bonding [D, D] pattern on the Hoogsteen face, but no natural nucleobase has an [A, A] pattern for base pair formation with **SA** (Fig. 5a). **SA** can interact with thymine using its Watson-Crick face in the *anti*-conformation; however, the resulting poor base-recognition-ability indicated that **SA** still adopted a syn conformation after photoirradiation due to the steric bulk around the 8-thio group. On the other hand, **SH** can interact with adenine using an [A, D] H-bonding pattern on the Hoogsteen face (Fig. S5).

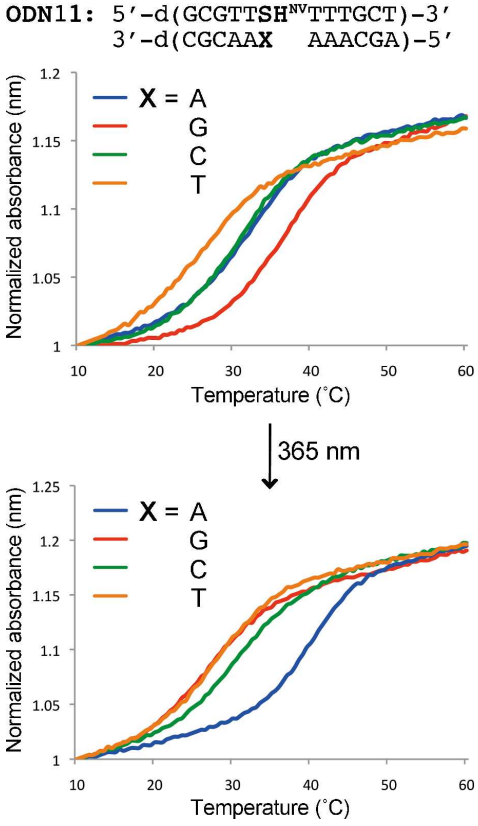

Fig. 4 Light-triggered changes in the denaturation profiles of duplexes containing ODN **11** determined by correlating absorbance at 260 nm vs. temperature. Conditions as given in Table 1.

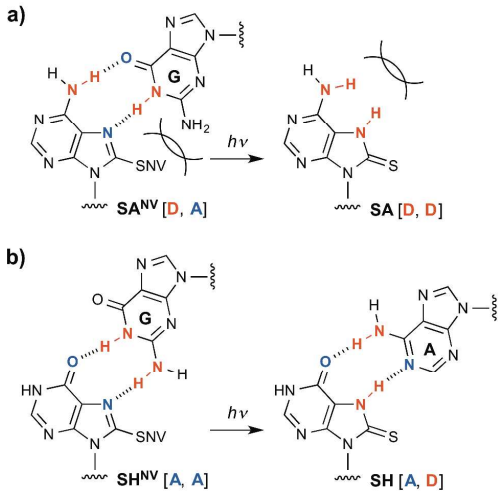

Fig. 5 Plausible change in base recognition by $\mathbf{SA}^{\mathbf{NV}}$ and $\mathbf{SH}^{\mathbf{NV}}$ upon photoirradiation.

Conclusions

In conclusion, we have developed 8-thiopurine nucleobase analogues bearing a photolabile NV group on the sulfur atom. The H-bonding patterns of the Hoogsteen face in $\mathbf{SA}^{\mathbf{NV}}$ and $\mathbf{SH}^{\mathbf{NV}}$ could be changed by photoirradiation. T_m analysis indicated that light-induced changes in the H-bonding pattern profoundly influence the base recognition ability of the nucleobase in duplex DNA. In particular, base recognition by $\mathbf{SH}^{\mathbf{NV}}$ is efficiently shifted from guanine to adenine upon photoirradiation. We believe that these unique light-responsive nucleobase analogues could be powerful tools for the spatiotemporal control of DNA assembly.

Experimental

General

Reagents and solvents were purchased from commercial suppliers and were used without purification unless otherwise specified. All experiments involving air- and/or moisture-sensitive compounds were carried out under an N_2 atmosphere. All reactions were monitored with analytical TLC (Merck Kieselgel 60 F254). Column chromatography was carried out using Fuji Silysia FL-100D. Physical data were measured as follows: NMR spectra were recorded on a JEOL JNM-ECS-400 spectrometer using $CDCl_3$ or DMSO-d_6 as the solvent with tetramethylsilane as an internal standard. IR spectra were recorded on a JASCO FT/IR-4200 spectrometer. Optical rotations were recorded on a JASCO P-2200 instrument. FAB mass spectra were measured on a JEOL JMS-700 mass spectrometer. MALDI-TOF mass spectra were recorded on a Bruker Daltonics Autoflex II TOF/TOF mass spectrometer.

Synthesis of the phosphoramidite-bearing $\mathbf{SA}^{\mathbf{NV}}$ and $\mathbf{SH}^{\mathbf{NV}}$ nucleobase analogues

6-Nitroveratrylthiol (2). To a solution of 6-nitroveratryl bromide (1.47 g, 5.36 mmol) in dry THF (54.0 mL) was added potassium thioacetate (734 mg, 6.43 mmol) and the reaction mixture was stirred for 5 h at room temperature. The solvent was removed *in vacuo* and the residue was partitioned between AcOEt and H_2O. The separated organic layer was washed with brine, then dried (Na_2SO_4) and concentrated *in vacuo*. The resulting residue (1.52 g) was dissolved in MeOH (51.0 mL) and 35% aqueous HCl (3.20 mL) was added. After being stirred for 12 h at 60 °C, the solvent was removed *in vacuo*. The residue was purified on a silica gel column eluted with hexane/AcOEt (4:1 to 1:1) to give **2** (1.15 g, 94%) as a yellow solid; Mp 86-87 ˚C; ^{1}H NMR (400 MHz, $CDCl_3$) δ 7.66 (1H, s), 6.86 (1H, s, H-2 or H-5), 4.03 (2H, d, J = 8.5 Hz, SCH_2Ar), 3.99 (3H,s, Ar-OCH_3), 3.95 (3H, s, Ar-OCH_3), 2.23 (1H, t, J = 8.5 Hz, SH); ^{13}C NMR (100 MHz, $CDCl_3$) δ 153.3, 147.8, 139.6, 132.0, 112.5, 108.2, 56.3, 56.2, 27.0; IR (KBr) 2577, 1520, 1273 cm^{-1}; FAB-LRMS m/z = 252 (MNa^+); FAB-HRMS calcd for $C_9H_{11}NNaO_4S$ 252.0306, found 252.0306.

6-*N*-Benzoyl-5'-*O*-(4,4'-dimethoxytrityl)-8-(6-nitroveratrylthio)-2'-deoxyadenosine (4). To a solution of **3**[23] (300 mg, 0.408 mmol) in dry DMF (4.10 mL) was added K_2CO_3 (169 mg, 1.22 mmol) and **2** (103 mg, 0.449 mmol) at room temperature. After being stirred for 1 h at room temperature, the resulting mixture was partitioned between Et_2O and H_2O. The separated organic layer was washed with brine, dried (Na_2SO_4) and concentrated *in vacuo*. The resulting residue was purified on a silica gel column eluted with hexane/AcOEt (2:3 to 1:2 with 0.5% Et_3N) to give **4** (187 mg, 52%) as a yellow foam; ^{1}H NMR (400 MHz, $CDCl_3$) δ 8.93 (1H, brs, NH), 8.43 (1H, s, H-2), 8.04 (2H, d, J = 7.5 Hz), 7.64-7.16 (14H, m), 6.77-6.73 (4H, m), 6.27 (1H, t, J = 7.0 Hz, H-1'), 4.99-4.85 (3H, m, H-3' and SCH_2Ar), 4.06 (1H, dd, J = 10.0 and 6.0 Hz, H-4'), 3.88 (3H, s, Ar-OCH_3), 3.76 (3H, s, Ar-OCH_3), 3.75 (3H, s, Ar-OCH_3), 3.71 (3H, s, Ar-OCH_3), 3.40-3.34 (3H, m, H-2'a and H-5'), 2.38 (1H, brs, OH), 2.33-2.26 (1H, m, H-2'b); ^{13}C NMR (100 MHz, $CDCl_3$) δ 164.7, 158.4, 158.4, 154.1, 153.2, 150.7, 148.4, 146.5, 144.7, 140.8, 135.9, 135.8, 133.8, 132.8, 130.0, 130.0, 128.9, 128.1, 128.0, 127.9, 127.8, 126.8, 123.7, 114.1, 113.0, 113.0, 108.0, 86.3, 85.7, 84.3, 72.8, 63.6, 56.4, 56.3, 55.2, 37.1, 33.6; IR (KBr) 1721 (C=O), 1521 (NO_2 as), 1274 (NO_2 sy) cm^{-1}; $[\alpha]_D^{22}$ -64.8 (c 1.00, $CHCl_3$); FAB-LRMS m/z = 885 (MH^+); FAB-HRMS calcd for $C_{47}H_{45}N_6O_{10}S$ 885.2918, found 885.2928.

6-*N*-Benzoyl-5'-*O*-(4,4'-dimethoxytrityl)-3'-*O*-(*N*,*N*-diisopropyl-β-cyanoethylphosphoramidyl)-8-(6-nitroveratrylthio)-2'-deoxyadenosine (5). To a suspension of **4** (150 mg, 0.17 mmol) in dry MeCN (1.7 mL) was added *N*,*N*-diisopropylethylamine (0.089 mL, 0.51 mmol) and 2-cyanoethyl-*N*,*N*'-diisopropylchlorophosphoramidite (0.057 mL, 0.26 mmol) at room temperature. After being stirred for 30 min, the resultant mixture was partitioned between AcOEt and H_2O. The separated organic layer was washed with saturated aqueous $NaHCO_3$, followed by brine, then dried (Na_2SO_4) and concentrated *in vacuo*. The residue was purified on a silica gel column eluted with hexane/AcOEt (3:2 with 0.5% Et_3N) to give **5** (142 mg, 77%) as a yellow foam; ^{31}P NMR δ 141.4, 141.1; FAB-LRMS m/z = 1085 (MH^+); FAB-HRMS calcd for $C_{56}H_{62}N_8O_{11}PS$ 1085.3996, found 1085.4053.

8-(6-Nitroveratrylthio)-2'-deoxyinosine (7). To a solution of **6**[24] (1.65 g, 5.00 mmol) in dry DMF (50.0 mL) was added K_2CO_3 (829 mg, 6.00 mmol) and **2** (1.37 g, 6.00 mmol) at room temperature. After being stirred for 24 h at room temperature, the solvent was removed *in vacuo*. The residue was purified on a silica gel column eluted with AcOEt to AcOEt/MeOH (10:1) to give **7** (596 mg, 25%) as a yellow powder; ^{1}H NMR (400 MHz, DMSO-d_6) δ 12.5 (1H, brs, NH), 8.02 (1H, s), 7.68 (1H, s), 7.47 (1H, s), 6.14 (1H, t, J = 6.5 Hz, H-1'), 5.33 (1H, brs, OH), 4.91 (1H, brs, OH), 4.79 and 4.75 (each 1H, each d, J = 13.5 Hz, SCH_2Ar), 4.37 (1H, brs, H-3'), 3.86 (3H, s, Ar-OCH_3), 3.85 (3H, s, Ar-OCH_3), 3.81-3.77 (1H, m, H-4'), 3.60-3.57 (1H, m, H-5'a),

3.46-3.44 (1H, m, H-5'b), 2.98-2.91 (1H, m, H-2'a), 2.12-2.06 (1H, m, H-2'b); ^{13}C NMR (100 MHz, DMSO-d_6) δ 155.6, 152.6, 149.5, 147.9, 146.5, 145.2, 139.7, 127.4, 124.7, 115.3, 108.3, 88.0, 84.3, 70.9, 61.9, 56.1, 56.1, 37.2, 34.1; IR (KBr) 3366, 1686, 1523, 1275 cm^{-1}; FAB-LRMS m/z = 480 (MH^+); FAB-HRMS calcd for $C_{19}H_{22}N_5O_8S$ 480.1189, found 480.1207.

5'-*O*-(4,4'-Dimethoxytrityl)-8-(6-nitroveratrylthio)-2'-deoxyinosine (8). To a solution of **7** (560 mg, 1.17 mmol) in dry pyridine (12.0 mL) was added 4,4'-dimethoxytrityl chloride (474 mg, 1.40 mmol) at room temperature. After being stirred for 5 h at room temperature, the reaction was quenched by addition of MeOH. The resultant mixture was partitioned between AcOEt and H_2O. The separated organic layer was washed with saturated aqueous $NaHCO_3$, followed by brine, then dried (Na_2SO_4) and concentrated *in vacuo*. The residue was purified on a silica gel column eluted with $CHCl_3$/MeOH (50:1 with 0.5% Et_3N) to give **8** (770 mg, 85%) as a yellow foam; ^{1}H NMR (400 MHz, $CDCl_3$) δ 7.70 (1H, s), 7.67 (1H, s), 7.53 (1H, s), 7.39 (1H, d, J = 7.5 Hz), 7.29-7.18 (1H, m), 6.78 (4H, dd, J = 8.5 and 3.0 Hz), 6.20 (1H, t, J = 6.5 Hz, H-1'), 4.95 and 4.91 (each 1H, each d, J = 13.5 Hz, SCH_2Ar), 4.76-4.74 (1H, m, H-3'), 4.02-3.99 (1H, m, H-4'), 3.97 (3H, s, Ar-OCH_3), 3.92 (3H, s, Ar-OCH_3), 3.77 (6H, s, 2 x Ar-OCH_3), 3.45-3.42 (1H, m, H-5'a), 3.35-3.31 (1H, m, H-5'b), 3.18-3.11 (1H, m, H-2'a), 2.30-2.23 (1H, m, H-2'b); ^{13}C NMR (100 MHz, $CDCl_3$) δ 158.4, 158.0, 153.1, 150.6, 150.0, 148.3, 144.6, 142.7, 139.9, 135.9, 130.0, 130.0, 128.2, 128.1, 127.7, 126.8, 124.9, 115.0, 113.0, 108.2, 86.3, 85.5, 84.2, 72.7, 63.8, 56.6, 56.3, 55.2, 37.5, 34.1; IR (KBr) 3007, 1678, 1519, 1276 cm^{-1}; FAB-LRMS m/z = 782 (MH^+); FAB-HRMS calcd for $C_{40}H_{40}N_5O_{10}S$ 782.2496, found 782.2531.

5'-*O*-(4,4'-Dimethoxytrityl)-3'-*O*-(*N*,*N*-diisopropyl-β-cyanoethylphosphoramidyl)-8-(6-nitroveratrylthio)-2'-deoxyinosine (9). To a solution of **8** (690 mg, 0.88 mmol) in dry MeCN (8.8 mL) was added *N*,*N*-diisopropylethylamine (0.46 mL, 2.7 mmol) and 2-cyanoethyl-*N*,*N*'-diisopropylchlorophosphoramidite (0.29 mL, 1.3 mmol) at room temperature. After being stirred for 30 min at room temperature, the resultant mixture was partitioned between AcOEt and H_2O. The separated organic layer was washed with saturated aqueous $NaHCO_3$, followed by brine, then dried (Na_2SO_4) and concentrated *in vacuo*. The residue was purified on a silica gel column eluted with hexane/AcOEt (1:4 with 0.5% Et_3N) to AcOEt:MeOH (10:1 with 0.5% Et_3N) to give **9** (600 mg, 74%) as a yellow foam; ^{31}P NMR δ 148.6, 148.4; FAB-LRMS m/z = 982 (MH^+); FAB-HRMS calcd for $C_{49}H_{57}N_7O_{11}PS$ 982.3574, found 982.3625.

Oligonucleotides synthesis

Solid-phase oligonucleotide synthesis was performed on an nS-8 Oligonucleotides Synthesizer (GeneDesign, Inc.) using commercially available reagents and phosphoramidites. The modified phosphoramidite was incorporated into the oligonucleotide with a coupling efficiency comparable to that of commercially available phosphoramidites without any modifications to the coupling conditions. Oligonucleotides were synthesized (with trityl-off) on a 500 Å CPG solid support column (0.2 μmol scale) using 5-(bis-3,5-trifluoromethylphenyl)-1*H*-tetrazole (0.25 M in MeCN) as the activator. Cleavage from the solid support and deprotection were accomplished with concentrated ammonium hydroxide solution at 55 °C for 12 h. The crude oligonucleotides were purified on a Nap 10 column (GE Healthcare) followed by RP-HPLC on a XBridge^{TM} OST C18 column, 2.5 μm, 10 x 50 mm (Waters) using MeCN in 0.1 M triethylammonium acetate buffer (pH 7.0). The purified oligonucleotides were quantified by UV absorbance at 260 nm and confirmed by MALDI-TOF mass spectrometry.

UV melting experiments

Melting temperatures (T_m) of the oligonucleotides were determined by measuring the change in absorbance at 260 nm as a function of temperature using a SHIMADZU UV-Vis spectrophotometer UV-1650PC equipped with a TMSPC-8 T_m analysis accessory. The samples were denatured at 100 °C and annealed slowly to room temperature. Absorbance was recorded in the forward and reverse direction between 5 and 90 °C at a rate of 0.5 °C/min. T_m values of duplexes after photoirradiation were measured using samples irradiated (365 nm) at 37 °C.

Photoirradiation reaction

Photoirradiation of oligonucleotides was performed in sodium phosphate buffer (pH 7.2) at 37 °C for 5 minutes using an OMRON UV-LED lamp ZUV-C30H as the light source (365 nm) and a ZUV-L10H as the lens unit (760 mW/cm^2). Analyses of the photoproducts were carried out without further purification.

Acknowledgement

This work was supported by the Japan Society for the Promotion of Science (JSPS), the Ministry of Education, Culture, Sports, Science and Technology (MEXT), and the Advanced Research for Medical Products Mining Programme of the National Institute of Biomedical Innovation (NIBIO), Japan.

Notes and references

[a] *Graduate School of Pharmaceutical Sciences, Osaka University, 1-6 Yamadaoka, Suita, Osaka 565-0871, Japan. Fax: +81 6-6879-8204; Tel: +81 6-6879-8200; E-mail: obika@phs.osaka-u,ac.jp*

[b] *National Institute of Biomedical Innovation (NIBIO), 7-6-8 Saito-Asagi, Ibaraki, Osaka 567-0085, Japan.*

[c] *Graduate School of Pharmaceutical Sciences, Nagoya University, Furo-cho, Chikusa-ku, Nagoya, Aichi 464-8601, Japan.*

† Electronic Supplementary Information (ESI) available: NMR spectra of new compounds, HPLC and MALDI-TOF MS analysis of modified ODNs, photoreaction of modified ODNs and UV melting curves for modified suplexes. See DOI: 10.1039/b000000x/

1 D. D. Young, H. Lusic, M. O. Lively, J. A. Yoder, A. Deiters, *ChemBioChem*, 2008, **9**, 2937.
2 D. D. Young, M. O. Lively, A. Deiters, *J. Am. Chem. Soc.*, 2010, **132**, 6183.
3 V. Mikat, A. Heckel, *RNA*, 2007, **13**, 2341.
4 J. M. Govan, D. D. Young, H. Lusic, Q. Liu, M. O. Lively, A. Deiters, *Nucleic Acids Res.*, in press.
5 A. Heckel, G. Mayer, *J. Am. Chem. Soc.*, 2005, **127**, 822.
6 C. Höbartner, S. K. Silverman, *Angew. Chem. Int. Ed.*, 2005, **44**, 7305.
7 A. Nierth, M. Singer, A. Jäschke, *Chem. Commun.*, 2010, **46**, 7975.
8 H. Lusic, D. D. Young, M. O. Lively, A. Deiters, *Org. Lett.*, 2007, **9**, 1903.
9 H. Lusic, M. O. Lively, A. Deiters, *Mol. BioSyst.*, 2008, **4**, 508.
10 K. B. Joshi, A. Vlachos, V. Mikat, T. Deller, A. Heckel, *Chem. Commun.*, 2012, **48**, 2746.
11 T. L. Schmidt, M. B. Koeppel, J. Thevarpadam, D. P. N. Goncalves, A. Heckel, *Small*, 2011, **7**, 2163.
12 A. Prokup, J. Hemphill, A. Deiters, *J. Am. Chem. Soc.*, 2012, **134**, 3810.
13 J. Hemphill, A. Deiters, *J. Am. Chem. Soc.*, 2013, **135**, 10512.

14 K. Morihiro, T. Kodama, R. Waki, S. Obika, *Chem. Sci.*, 2014, **5**, 744.
15 A. Patchornik, B. Amit, R. B. Woodward, *J. Am. Chem. Soc.*, 1970, **92**, 6333.
16 M. L. Hamm, R. Cholera, C. L. Hoey, T. J. Gill, *Org. Lett.*, 2004, **6**, 3817.
17 K. Miyata, R. Tamamushi, H. Tsunoda, A. Ohkubo, K. Seio, M. Sekine, *Org. Lett.*, 2009, **11**, 605-608.
18 T. P. Prakash, R. K. Kumer, K. N. Ganesh, *Tetrahedron*, 1993, **49**, 4035.
19 R. E. Holmes, R. K. Robins, *J. Am. Chem. Soc.*, 1964, **86**, 1242.
20 I. V. Kutyavin, R. L. Rhinehart, E. A. Lukhtanov, V. V. Gorn, R. B. Meyer, Jr., H. B. Gamper, Jr., *Biochemistry*, 1996, **35**, 11170.
21 J. Lohse, O. Dahl, P. E. Nielsen, *Proc. Natl. Acad. Sci. USA*, 1999, **96**, 11804.
22 G. Varani, W. H. McClain, *EMBO Reports*, 2000, **1**, 18.

Table of contents entry

Photoinduced change in hydrogen bonding pattern has a strong effect on base recognition by nucleobase analogues.